Security Constrained DC OPF Considering Generator Responses

Minyue Ma, *Student Member, IEEE*, Lingling Fan, *Senior Member, IEEE*

Abstract

Considering generator responses after contingencies provides a more practical solution to security constrained direct current optimal power flow (DCOPF) problems. The major difficulty of solving such OPF includes the large number of contingencies and non-convexity of the generator response constraints. In the literature, mixed-integer linear programming (MILP) formulation relying on big-M technique has been applied to deal with the non-convexity of generator response constraints. In this paper, we further improve the solving speed by formulating generator response constraints via bilinear expressions and adopting Benders' decomposition technique to decompose the problem into a master problem and multiple subproblems, with each subproblem associated with a contingency. Benders' decomposition strategies were investigated in this research to seek an efficient decomposition approach. Through preserving bilinear expressions related to the base case power while relaxing the rest bilinear expressions via McCormick envelops, we designed an efficient Benders' decomposition strategy. Case study results demonstrate the efficiency of the proposed formulation compared to the state-of-the-art formulations.

Index Terms

Security constrained optimal power flow; Generator response; Benders' decomposition; Bilinear formulation; Mixed integer programming.

I. Introduction

SECURITY constrained OPF (SCOPF) [**?**] is an extension of OPF. In general, its purpose is to find an operation point to optimize an objective function at base case, while satisfying all pre-contingency (base case) constraints and post-contingency constraints. The particular type investigated in this paper is preventive SCOPF [**?**], i.e., except automatic control of generators (AGC), rescheduling will not be considered.

In conventional formulation of preventive security constrained OPF, either contingencies related to generator outages are ignored [**?**], [**?**], [**?**], or the same operating conditions are assumed for generators (except the one at the slack bus) in the pre- and post-contingency [**?**], [**?**]. On the other hand, in practical situations, generator outages are common and the system may assume a very different response compared to that related to line outages [**?**]. With generator outages, online generators need to be re-dispatched to compensate power loss. Their responses are governed by their automatic generator control (AGC) setting.

A generator's post-contingency response is illustrated in Fig. 1, where $P_{gi}^{\max}$ and $P_{gi}^{\min}$ are the upper and lower limits of the ith generator's active power output respectively; $P_{gi}^{(0)}$ is the power in pre-contingency state; $P_{gi}^{(k)}$ is the power in post-contingency state; $\Delta^{(k)}$ is the active power imbalance in the system right after the contingency before AGC; $\alpha_i^{(k)}$ is the participation factor corresponding to the slope. For each generator, its participation factor is the ratio of the output power change of this generator against the the total power change. Three feasible regions are denoted in the Fig. 1.

M. Ma, and L. Fan are with Department of Electrical Engineering at University of South Florida, Tampa, FL 33620 (Email: `linglingfan@usf.edu`)

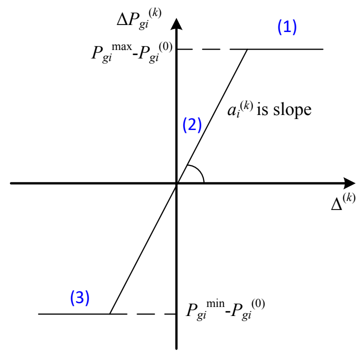

Fig. 1. Generator post-contingency response.

There are existing works that have considered generator outages and AGC in preventive SCOPF, e.g., [**?**], [**?**], [**?**]. In [**?**], [**?**], [**?**], preventive SCOPF is formulated based on the DC power flow model. Generator outages are considered in these works and the generator responses based on AGC in post-contingency are assumed to be always follow their predefined participation factors, i.e. only region (2) is considered. Contingency constraints have also been considered in alternating current optimal power flow (ACOPF) problems, e.g., [**?**], [**?**]. However, for the generator responses of contingencies, AGC is either not modeled [**?**] or only partially modeled by considering only region (2) [**?**]. The formulations in these works could simplify the problem as the generator responses are defined by a set of linear constraints. However, due to the inaccurate representation of the feasible region, the solutions are not practical.

To model AGC accurately, binary variables have to be introduced. A mixed-integer programming (MIP) formulation is designed in [**?**] and [**?**]. The generator response constraint is formulated as a set of mixed-integer linear programming (MILP) constraints based on big-M technique. The major disadvantage of this method is the well-known disadvantage related to big-M formulation , i.e., the difficulty of finding a suitable value M.

Another major challenge to solve SCOPF with generator response constraints is the large size of the problem. Even we only consider the "N-1" criterion, the computation cost of the SCOPF with all contingencies considered could be too high. To address this issue, decomposition techniques, e.g., alternating direction method of multipliers (ADMM) and Benders' decomposition, have been implemented to reduce the computing cost as shown in [**?**] for corrective AC-SCOPF.

For example, alternating direction method of multipliers (ADMM)-based decomposition is adopted in [**?**] to decompose the security constrained DCOPF (DC-SCOPF) problem into independent subproblems for each pre-contingency and post-contingency case. Based on this algorithm, the SCOPF can be computed in parallel by distributed agents. In [**?**], an ADMM based proximal message passing algorithm is developed for DC-SCOPF. The original SCOPF is decomposed based on individual devices and their associated base-case and contingency scenarios. Thus, all devices update their variables in parallel, and each contingency scenario of the device can update its variables in parallel as well, except the generators. This algorithm has been extended in [**?**] to solve an SCOPF while considering the primary frequency response of generator. To avoid the non-convex characteristic of the generator responses, only region (2) is considered in [**?**]. ADMM is also found to be applied to security constrained ACOPF problem after convex relaxation in [**?**].

Benders' decomposition is a widely adopted method in power system optimization problems. It has been used to solve AC-

SCOPF problems in 1987 [?]. In [?], an SCOPF problem is decomposed into one master problem and multiple subproblems, each associated with a contingency. The SCOPF considered in [?] is a corrective SCOPF; thus AGC is not modeled. Through retaining the optimal power flow structure of subproblems, the computation efficiency of the algorithm of [?] can be improved [?]. Further, [?] shows that the Benders cuts should be created with care to achieve computing efficiency. Finally, in [?], Benders' decomposition is implemented to solve a preventive DC-SCOPF with AGC formulated as linear constraints associated with binary variables.

The ADMM methods are heuristic methods to handle non-convexity and the solution from ADMM does not guarantee a global optimum. Hence, our paper focuses on investigating a more efficient MIP formulation and the corresponding solving strategy.

Our Contributions: The contribution of this paper is two-fold. (i) A bilinear MIP formulation is designed to model generator post-contingency responses. The proposed model accurately represents the generator response characteristics. (ii) An efficient Benders' decomposition is designed to decompose the bilinear MIP problem. Various Benders' decomposition strategies were investigated in this research. Through preserving bilinear expressions related to the base case power generation while relaxing the rest bilinear expressions via McCormick envelops, we designed a Benders' decomposition strategy that yields to efficient solving. The resulting MIP formulation and the solving strategy enable better computing efficiency compared to the MILP formulation presented in [?], [?].

The remainder of the paper is organized as follows. In Section II, we introduce SCOPF and the MILP formulation of the generator response constraints. The proposed bilinear formulation and two Benders' decomposition strategies are described in Section III. Case study is presented in Section IV. Conclusion is presented in Section V.

II. Preventive DC-SCOPF formulation

The mathematic formulation of security constrained DCOPF is as follows.

$$\min_{x^{(0)},x^{(k)},u^{(0)}} \quad f_0(x^{(0)},u^{(0)}) \tag{1a}$$

$$s.t. \quad g^{(k)}(x^{(k)},u^{(k)})=0 \qquad k\in\mathcal{C} \tag{1b}$$

$$h^{(k)}(x^{(k)},u^{(k)})\le 0 \qquad k\in\mathcal{C} \tag{1c}$$

where x refers to dc power flow state variables: bus voltage phase angles at each scenario and u refers to the control variables: active power dispatch of each generator. N_c is the total number of contingencies and $\mathcal{C}=\{0,1,\cdots,N_c\}$ is the set for the index of scenarios. If $k=0$, the correspond constraints and variables belong to the base case (pre-contingency).

The decision variables of SCOPF are the base case control actions $u^{(0)}$, state variables $x^{(0)}$ and contingency case state variables $x^{(k)}$.

The objective function is the total operation cost. Denote the cost coefficients as C_{2i},C_{1i},C_{0i}, the objective function could be defined as:

$$f_0=\sum_{i\in\mathcal{G}_{on}} C_{2i}(P_{gi}^{(0)})^2+C_{1i}P_{gi}^{(0)}+C_{0i}$$

where $P_{gi}^{(0)}$ is the i-th generator's active power dispatch in base case and $\mathcal{G}_{on}$ notates the set of online generators.

The equality (g) and inequality constraints (h) are explained as follows.

A. Equality constraints: power flow equations

The following constraints are enforced on all bus $i \in \mathcal{N}$ for base case and post-contingency scenarios:

$$P_{gi}^{(0)} - P_{di}^{(0)} = \sum_{(i,j)\in\mathcal{L}} B_{ij}(\theta_i^{(0)} - \theta_j^{(0)}) \qquad i \in \mathcal{N} \tag{2}$$

$$P_{gi}^{(k)} - P_{di}^{(k)} = \sum_{(i,j)\in\mathcal{L}_k} B_{ij}(\theta_i^{(k)} - \theta_j^{(k)}) \qquad i \in \mathcal{N} \tag{3}$$

where $\mathcal{L}$ and $\mathcal{L}_k$ are the sets of transmission lines in base case and post-contingency scenarios; $P_{gi}^{(k)}$ is the generator active power dispatch in post-contingency scenarios; $P_{di}^{(k)}$ is the load at bus i; B_{ij} is the susceptance of the transmission line from bus i to bus j; θ_i is the voltage phase angle of bus i.

B. Inequality constraints: component limits

Inequality constraints include transmission line limits, generator power limits, and others. Eqs. (4) and (5) notate transmission line flow limits. Eqs. (6) and (7) notate generator power limits. Eqs. (8) and (9) enforce the reference bus angle to zero.

$$|B_{ij}(\theta_i^{(0)} - \theta_j^{(0)})| \leq F_{ij}^{\max} \qquad (i,j) \in \mathcal{L} \tag{4}$$

$$|B_{ij}(\theta_i^{(k)} - \theta_j^{(k)})| \leq F_{ij}^{\max} \qquad (i,j) \in \mathcal{L}_k \tag{5}$$

$$P_{gi}^{\min} \leq P_{gi}^{(0)} \leq P_{gi}^{\max} \qquad i \in \mathcal{G}_{on}^{(0)} \tag{6}$$

$$P_{gi}^{\min} \leq P_{gi}^{(k)} \leq P_{gi}^{\max} \qquad i \in \mathcal{G}_{on}^{(k)} \tag{7}$$

$$\theta_{\text{ref}}^{(0)} = 0 \tag{8}$$

$$\theta_{\text{ref}}^{(k)} = 0 \tag{9}$$

where $\mathcal{G}_{on}^{(0)}$ and $\mathcal{G}_{on}^{(k)}$ are the sets of online generators in base case and post-contingency scenarios; $F_{ij}^{\max}$ is the maximum transmission line capacity; $P_{gi}^{\min}$ and $P_{gi}^{\max}$ are the lower and upper limits of generator active power output; θ_{ref} means the reference bus voltage phase angle.

C. Generator post-contingency response constraints

When there is a generator outage, the rest of the generators will adjust their outputs based on their participation factors to make up the lost power. If the total load keeps constant, the load variation is zero. Thus, the definition of $\Delta^{(k)}$ has to be carefully designed to consider both load variation contingency and generator outage (while load being constant) contingency.

Hence, $\Delta^{(k)}$ is defined as total generation change for the set of online generators at kth contingency.

$$\Delta^{(k)} = \sum_{i\in\mathcal{G}_{on}^{(k)}} P_{gi}^{(k)} - \sum_{i\in\mathcal{G}_{on}^{(k)}} P_{gi}^{(0)} \tag{10}$$

$$P_{gi}^{(k)} = P_{gi}^{(0)} + \alpha_i^{(k)} \Delta^{(k)} \tag{11}$$

where $\mathcal{G}_{on}^{(k)} \subseteq \mathcal{G}$ is the set of all online generators at kth contingency, α is the participation factor and

$$\sum_{i \in \mathcal{G}_{on}^{(k)}} \alpha_i^{(k)} = 1. \tag{12}$$

Considering the output limit of generators, (11) can not always be complied by generators. If $P_{gi}^{(0)} + \alpha_i^{(k)} \Delta^{(k)}$ is lower than the minimum limit or greater than the maximum limit, generator should dispatch at its minimum or the maximum at this contingency. The response of the generator can be illustrated in Fig. 1.

Moreover, according to [**?**], these three regions can be described as a piecewise function:

$$\text{Region (1)}: \; P_{gi}^{(k)} = P_{gi}^{\max} \tag{13a}$$

$$\text{and } P_{gi}^{(k)} \leq P_{gi}^{(0)} + \alpha_i^{(k)} \Delta^{(k)} \tag{13b}$$

$$\text{Region (2)}: \; P_{gi}^{\min} \leq P_{gi}^{(k)} \leq P_{gi}^{\max} \tag{13c}$$

$$\text{and } P_{gi}^{(k)} = P_{gi}^{(0)} + \alpha_i^{(k)} \Delta^{(k)} \tag{13d}$$

$$\text{Region (3)}: \; P_{gi}^{(k)} = P_{gi}^{\min} \tag{13e}$$

$$\text{and } P_{gi}^{(k)} \geq P_{gi}^{(0)} + \alpha_i^{(k)} \Delta^{(k)}. \tag{13f}$$

The constraints (13) mean that in general, the generator active power output $P_{gi}^{(k)}$ will follow its participation factor so that the generator is working in Region (2) until $P_{gi}^{(k)}$ hits its upper or lower limit. If $P_{gi}^{(k)}$ violates its upper limit, the generator should settle at the upper limit or Region (1). If $P_{gi}^{(k)}$ violates its lower limit, the generator should settle at the lower limit or Region (3).

If all generators comply with the above constraints, the problem may be infeasible. Below is an example. For a system with three generators, assume that the post-contingency generation of G1 is hitting the upper limit and settles in Region (1), while the rest generators are in Region (2). That is, $P_{g1}^{(k)} = P_{g1}^{\max} < P_{g1}^{(0)} + \alpha_1^{(k)} \Delta^{(k)}$, and the other two generators follow the following relationship: $P_{gi}^{(k)} = P_{gi}^{(0)} + \alpha_i^{(k)} \Delta^{(k)}$. In this situation, $\sum P_{gi}^{(k)} - \sum P_{gi}^{(0)} < \Delta^{(k)}$. So that the power imbalance can not be fully compensated. To avoid this situation, we set a reference generator in the system. Excepting the limit constraint (13c), the rest constraints of (13) are not enforced on this generator.

D. The MILP formulation

The piecewise function (13) is nonconvex. The set of constraints can be formulated via big-M technique into an MILP formulation, as shown in [**?**] [**?**]. In the following, the formulation is briefly introduced. Since there are three regions, two binary variables are introduced: $\omega_{1i}^{(k)}$ (1 for max limit hitting; 0 for otherwise) and $\omega_{2i}^{(k)}$ (1 for min limit hitting; 0 for otherwise).

Hence, Region (1) is be represented by $(\omega_{1i}^{(k)}, \omega_{2i}^{(k)}) = (1, 0)$, Region (2) $(\omega_{1i}^{(k)}, \omega_{2i}^{(k)}) = (0, 0)$ and Region (3): $(\omega_{1i}^{(k)}, \omega_{2i}^{(k)}) =$

$(0, 1)$.

$$P_{gi}^{\min} \leq P_{gi}^{(k)} \leq P_{gi}^{\max} \tag{14a}$$

$$P_{gi}^{\max} - P_{gi}^{(k)} \leq (1 - \omega_{1i}^{(k)})M \tag{14b}$$

$$P_{gi}^{(k)} - P_{gi}^{\min} \leq (1 - \omega_{2i}^{(k)})M \tag{14c}$$

$$P_{gi}^{(k)} \leq P_{gi}^{(0)} + \alpha_i^{(k)}\Delta^{(k)} + \omega_{2i}^{(k)}M \tag{14d}$$

$$P_{gi}^{(k)} \geq P_{gi}^{(0)} + \alpha_i^{(k)}\Delta^{(k)} - \omega_{1i}^{(k)}M \tag{14e}$$

$$\omega_{1i}^{(k)} + \omega_{2i}^{(k)} \leq 1$$

$$\omega_{1i}^{(k)}, \omega_{2i}^{(k)} \in \{0, 1\}$$

- $(\omega_{1i}^{(k)}, \omega_{2i}^{(k)}) : (1, 0)$, (14) is equivalent to (13a) & (13b);
- $(\omega_{1i}^{(k)}, \omega_{2i}^{(k)}) : (0, 0)$, (14) is equivalent to (13c) & (13d);
- $(\omega_{1i}^{(k)}, \omega_{2i}^{(k)}) : (0, 1)$, (14) is equivalent to (13e) & (13f).

M is a large constant number. This method is easy to implement, but there is no guarantee to find an appropriate value for M. If M is too small, the equivalent relation between (13) and (14) may not hold. If M is too large, it may cause numerical instability for computation.

Based on the MILP formulation, Benders' decomposition has been proposed in [**?**].

III. The proposed bilinear formulation

In this section, we will first provide the bilinear formulation which is equivalent to constraints (13). Benders' decomposition strategies are then examined.

A. Bilinear formulation for generator response

Based on the definition of ω_{1i} and ω_{2i} in (14), the bilinear formulation for constraints (13) can be expressed as follows:

$$P_{gi}^{\min} \leq P_{gi}^{(k)} \leq P_{gi}^{\max} \tag{15a}$$

$$\omega_{1i}^{(k)}(P_{gi}^{(k)} - P_{gi}^{\max}) \geq 0 \tag{15b}$$

$$\omega_{2i}^{(k)}(P_{gi}^{\min} - P_{gi}^{(k)}) \geq 0 \tag{15c}$$

$$(1 - \omega_{2i}^{(k)})(P_{gi}^{(k)} - P_{gi}^{(0)} - \alpha_i^{(k)}\Delta^{(k)}) \leq 0 \tag{15d}$$

$$(1 - \omega_{1i}^{(k)})(P_{gi}^{(k)} - P_{gi}^{(0)} - \alpha_i^{(k)}\Delta^{(k)}) \geq 0 \tag{15e}$$

$$\omega_{1i}^{(k)} + \omega_{2i}^{(k)} \leq 1 \tag{15f}$$

$$\omega_{1i}^{(k)}, \omega_{2i}^{(k)} \in \{0, 1\} \tag{15g}$$

Directly solving the SCOPF problem with constraints (15) is difficult since there are bilinear terms consisting of binary variables. Therefore, we seek Benders' decomposition strategies.

B. Benders' decomposition: Approach 1

The first strategy of Benders' decomposition follows the decomposition structure shown in Fig. 2. The master problem will decide the base case generator dispatch as well as binary variables for the base case and all contingency scenarios. With the binary variables given, the subproblems associated with contingencies are linear programming problems. Their decision variables are continuous variables.

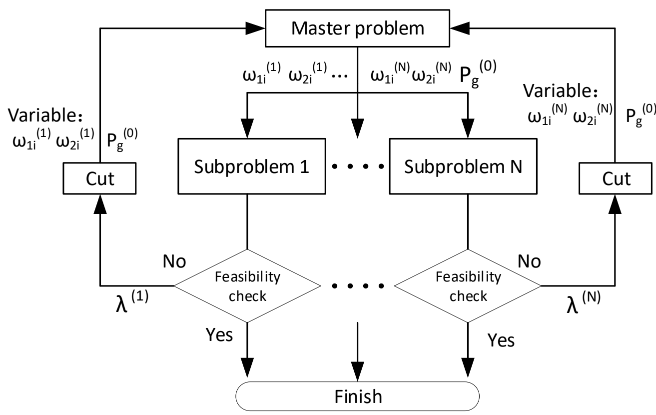

Fig. 2. Flow chart of Benders' decomposition Approach 1.

Compared with the MILP formulation which can be directly solved by off-shelf solvers, Approach 1 shows obvious worse performance on both of the solution quality and computation efficiency. A brief comparison on the 5-bus system and 39-bus system are shown in Table I.

The disadvantages of Approach 1 appear to be caused by the Benders' cuts associated with both of the binary and continuous variables. Subproblems generate many infeasible solutions and cuts. So the problem needs many iterations. Moreover, each iteration will add at least one constraint associated to a binary variable to the master problem. The complexity of the master problem could be increased significantly along with iterations.

TABLE I
COMPARISON BIG-M MILP PROBLEM SOLVING USING MOSEK AND APPROACH 1.

		Big-M		Direct Benders		
Case	# of contingencies	Time	Obj	Time	Obj	Iterations
Case5	1	0.25	21703.48	6.09	21703.48	13
	2	0.27	21703.48	9.11	21786.09	17
Case39	1	0.16	41285.97	5.31	41493.44	10
	2	0.72	41298.97	14.95	41569.21	18

C. Benders' Decomposition: Approach 2

1) McCormick envelopes of the bilinear formulation: To avoid the issue of Approach 1, we re-design Benders' decomposition to reduce the "coupling" between the master problem and the subproblems.

Fig. 3 presents the new decomposition method: Approach 2. In this new design, the decision variables of the master problem are only associated with the base case. The base case power dispatch $P_{gi}^{(0)}$ will be passed to each subproblem associated with each contingency. Each subproblem will decide the power dispatch and guarantee that the post-contingency generator response constraints are satisfied.

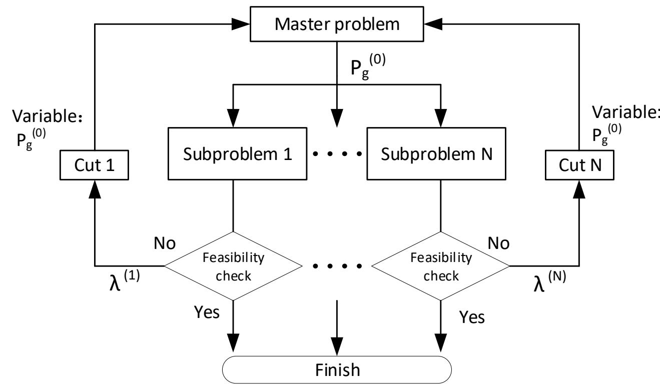

Fig. 3. Flow chart for Benders' Decomposition: Approach 2.

Examining the bilinear formulation (15), it can be found that the subproblem for k-th contingency has to deal with four constraints with bilinear components: (15b)-(15e). Four bilinear expressions exist: $\omega_{1i}^{(k)}P_{gi}^{(k)}$, $\omega_{2i}^{(k)}P_{gi}^{(k)}$, $\omega_{1i}^{(k)}\Delta^{(k)}$, and $\omega_{2i}^{(k)}\Delta^{(k)}$.

We implement McCormick envelopes to linearize the four bilinear terms so that the subproblems are MILP problems. According to [**?**], the linearization based on the McCormick envelopes should be tighter than the big-M based linearization. Its efficiency has been validated through implementation on unit commitment and chance constrained problems in [**?**] and [**?**].

The process for the bilinear formulation linearization based on the McCormick envelopes is presented as follows. Considering a general bilinear term $\{xy|x^{\min} \leq x \leq x^{\max}, y^{\min} \leq y \leq y^{\max}\}$, its McCormick envelops is:

$$z = xy$$

$$z \geq x^{\min}y + xy^{\min} - x^{\min}y^{\min} \tag{16a}$$

$$z \geq x^{\max}y + xy^{\max} - x^{\max}y^{\max} \tag{16b}$$

$$z \leq xy^{\max} + x^{\min}y - x^{\min}y^{\max} \tag{16c}$$

$$z \leq x^{\max}y + xy^{\min} - x^{\max}y^{\min} \tag{16d}$$

Therefore, to linearize (15), we first define:

$$\overline{P}_{gi}^{(k)} = \omega_{1i}^{(k)}P_{gi}^{(k)} \tag{17}$$

$$\underline{P}_{gi}^{(k)} = \omega_{2i}^{(k)}P_{gi}^{(k)} \tag{18}$$

$$\overline{\Delta}^{(k)} = \omega_{1i}^{(k)}\Delta^{(k)} \tag{19}$$

$$\underline{\Delta}^{(k)} = \omega_{2i}^{(k)}\Delta^{(k)} \tag{20}$$

The upper and lower bound of $P_{gi}^{(k)}$ are $P_{gi}^{\max}$ and $P_{gi}^{\min}$. $\omega_{1i}^{(k)}$ and $\omega_{2i}^{(k)}$ are binary variables which means their upper and lower limit is 1 and 0 respectively. For $\Delta^{(k)}$, we have $\Delta_{\max}^{(k)} = P_{gk}^{\max}$, $\Delta_{\min}^{(k)} = P_{gk}^{\min}$ for generator outage scenarios, where $P_{gk}^{\max}$ and $P_{gk}^{\min}$ are the output limits of the failure generator. Assuming $P_{gi}^{\min} = 0$ in general, the McCormick envelops for

(17)-(20) can be expressed as follows:

$$\begin{cases} 0 \leq \overline{P}_{gi}^{(k)} \leq \omega_{1i}^{(k)} P_{gi}^{\max} \\ P_{gi}^{(k)} - (1-\omega_{1i}^{(k)}) P_{gi}^{\max} \leq \overline{P}_{gi}^{(k)} \leq P_{gi}^{(k)} \end{cases} \tag{21}$$

$$\begin{cases} 0 \leq \underline{P}_{gi}^{(k)} \leq \omega_{2i}^{(k)} P_{gi}^{\max} \\ P_{gi}^{(k)} - (1-\omega_{2i}^{(k)}) P_{gi}^{\max} \leq \underline{P}_{gi}^{(k)} \leq P_{gi}^{(k)} \end{cases} \tag{22}$$

$$\begin{cases} 0 \leq \overline{\Delta}^{(k)} \leq \omega_{1i}^{(k)} \Delta_{\max}^{(k)} \\ \Delta^{(k)} - (1-\omega_{1i}^{(k)}) \Delta_{\max}^{(k)} \leq \overline{\Delta}^{(k)} \leq \Delta^{(k)} \end{cases} \tag{23}$$

$$\begin{cases} 0 \leq \underline{\Delta}^{(k)} \leq \omega_{2i}^{(k)} \Delta_{\max}^{(k)} \\ \Delta^{(k)} - (1-\omega_{2i}^{(k)}) \Delta_{\max}^{(k)} \leq \underline{\Delta}^{(k)} \leq \Delta^{(k)} \end{cases} \tag{24}$$

Further, (15)(b)-(e) can be expressed as follows.

$$\omega_{1i}^{(k)} P_{gi}^{\max} - \overline{P}_{gi}^{(k)} \leq 0 \tag{25}$$

$$\underline{P}_{gi}^{(k)} - \omega_{2i}^{(k)} P_{gi}^{\min} \leq 0 \tag{26}$$

$$(P_{gi}^{(k)} - \underline{P}_{gi}^{(k)}) - (1-\omega_{2i}^{(k)}) P_{gi}^{(0)} - \alpha_i^{(k)} (\Delta^{(k)} - \underline{\Delta}^{(k)}) \leq 0 \tag{27}$$

$$(1-\omega_{1i}^{(k)}) P_{gi}^{(0)} + \alpha_i^{(k)} (\Delta^{(k)} - \overline{\Delta}^{(k)}) - (P_{gi}^{(k)} - \overline{P}_{gi}^{(k)}) \leq 0 \tag{28}$$

In the above formulation, we do not linearize terms $\omega_{1i}^{(k)} P_{gi}^{(0)}$ and $\omega_{2i}^{(k)} P_{gi}^{(0)}$. The reason is that $P_{gi}^{(0)}$ will be determined by the master problem. In subproblems, $P_{gi}^{(0)}$ is treated as a constant.

2) Benders' decomposition: Based on aforementioned definition, the **subproblem** could be formulated as:

$$v^{(k)} := \min \quad ||[s_{1i}^{(k)}, s_{2i}^{(k)}, s_3^{(k)}]|| \tag{29a}$$

$s.t.$ Power flow constraints: (3), (5), (7), (9)

Generator limits: (15a)

McCormick envelop constraints: (21) $\sim$ (26)

$$(P_{gi}^{(k)} - \underline{P}_{gi}^{(k)}) - (1-\omega_{2i}^{(k)}) \hat{P}_{gi}^{(0)} - \alpha_i^{(k)} (\Delta^{(k)} - \underline{\Delta}^{(k)}) \leq s_{1i}^{(k)} \tag{29b}$$

$$(1-\omega_{1i}^{(k)}) \hat{P}_{gi}^{(0)} + \alpha_i^{(k)} (\Delta^{(k)} - \overline{\Delta}^{(k)}) - (P_{gi}^{(k)} - \overline{P}_{gi}^{(k)}) \leq s_{2i}^{(k)} \tag{29c}$$

$$\sum_{i \in \mathcal{G}_{on}^{(k)}} P_{gi}^{(k)} - \sum_{i \in \mathcal{G}_{on}^{(k)}} \hat{P}_{gi}^{(0)} - \Delta^{(k)} = s_3^{(k)} \tag{29d}$$

$$s_{1i}^{(k)}, s_{2i}^{(k)} \geq 0 \tag{29e}$$

Binary variable constraints: (15f), (15g) where $\hat{P}_{gi}^{(0)}$ is a known value passed from the master problem, $s_{1i}^{(k)}$, $s_{2i}^{(k)}$, $s_3^{(k)}$ are slack variables to relax region (2) constraints defined by (27), (28) as well as the Δ^k definition constraint (10).

$v^{(k)}$ is the value of the objective function (29a). Obviously when $v^{(k)} = 0$, the solution of the master problem $\hat{P}_{gi}^{(0)}$ is feasible for the contingency cases. In the computing process, we consider $\hat{P}_{gi}^{(0)}$ is feasible for the contingency cases if $v^{(k)} \leq \epsilon$, where ϵ is a predefined small constant value.

To generate Benders' cuts, we need to know the dual variable of constraints (29d), (29b) and (29c). However, because there are binary variables included in (29b) and (29c), we can not directly obtain dual variables from the subproblem (29).

To solve this issue, we implement a technique introduced in [**?**]. The process of this technique is described as follows.

- First, we solve the subproblem (29) to obtain the binary decision variables $\omega_{1i}^{(k)}$, $\omega_{2i}^{(k)}$. Denote these value as $\hat{\omega}_{1i}^{(k)}$ and $\hat{\omega}_{2i}^{(k)}$.
- Next, replace $\omega_{1i}^{(k)}$ and $\omega_{2i}^{(k)}$ by $\hat{\omega}_{1i}^{(k)}$ and $\hat{\omega}_{2i}^{(k)}$ in (29), and solve the problem.

The new formulation of the subproblem can be expressed as follows.

$$
\begin{aligned}
v^{(k)} := \min \quad & ||[s_{1i}^{(k)}, s_{2i}^{(k)}, s_3^{(k)}]|| && \text{(30a)}\\
s.t. \quad & \text{Power flow constraints: (3), (5), (7), (9)} \\
& \text{Generator limits: (15a)} \\
& \text{McCormick envelop constraints: (21)} \sim \text{(26)} \\
\lambda_{1i}^{(k)} \, : & (P_{gi}^{(k)} - \underline{P}_{gi}^{(k)}) - (1 - \hat{\omega}_{2i}^{(k)})\hat{P}_{gi}^{(0)} - \alpha_i^{(k)}(\Delta^{(k)} - \underline{\Delta}^{(k)}) \leq s_{1i}^{(k)} && \text{(30b)}\\
\lambda_{2i}^{(k)} \, : & (1 - \hat{\omega}_{1i}^{(k)})\hat{P}_{gi}^{(0)} + \alpha_i^{(k)}(\Delta^{(k)} - \overline{\Delta}^{(k)}) - (P_{gi}^{(k)} - \overline{P}_{gi}^{(k)}) \leq s_{2i}^{(k)} && \text{(30c)}\\
\lambda_3^{(k)} : & \sum_{i \in \mathcal{G}_{on}^{(k)}} P_{gi}^{(k)} - \sum_{i \in \mathcal{G}_{on}^{(k)}} \hat{P}_{gi}^{(0)} - \Delta P^{(k)} = s_3^{(k)} && \text{(30d)}\\
& s_{1i}^{(k)}, s_{2i}^{(k)} \geq 0 && \text{(30e)}
\end{aligned}
$$

Because of the characteristics of the binary decision variables, $\omega_{1i}^{(k)}$ and $\omega_{2i}^{(k)}$, the constraints (15a) and (21) $\sim$ (28) are equivalent to (15). It means the solutions to the McCormick envelops in this case are always feasible for the original problem.

Take the example when $\omega_{1i}^{(k)} = 1$ and $\omega_{2i}^{(k)} = 0$. The constraint group (15) can be expressed as:

$$
\begin{aligned}
& P_{gi}^{\min} \leq P_{gi}^{(k)} \leq P_{gi}^{\max} \\
& P_{gi}^{(k)} - P_{gi}^{\max} \geq 0 \\
& P_{gi}^{(k)} - P_{gi}^{(0)} - \alpha_i^{(k)}\Delta^{(k)} \leq 0
\end{aligned}
$$

The McCormick envelop constraints (21) $\sim$ (24) lead to the following equality constraints: $P_{gi}^{(k)} = \overline{P}_{gi}^{(k)}$, $\underline{P}_{gi}^{(k)} = 0$, $\Delta^{(k)} = \overline{\Delta}^{(k)}$, $\underline{\Delta}^{(k)} = 0$. Based on these equality constraints, the constraints (25) $\sim$ (28) can be converted to:

$$
P_{gi}^{(k)} - P_{gi}^{\max} \geq 0
$$

$$P_{gi}^{(k)} - P_{gi}^{(0)} - \alpha_i^{(k)}\Delta^{(k)} \leq 0$$

Thus, for $\omega_{1i}^{(k)} = 1$ and $\omega_{2i}^{(k)} = 0$, the McCormick constraints (21) $\sim$ (28) along with the power limit constraint (15a) are equivalent to (15). Thus the feasible region of the McCormick envelops and the feasible region of the original problem are the same because of the binary decision variables.

Based on the solution of (30), the feasibility cut is shown as follows:

$$\begin{aligned} 0 \geq & \hat{v}^{(k)} - \hat{\lambda}_3^{(k)} \sum_{i \in \mathcal{G}_{on}} (P_{gi}^{(0)} - \hat{P}_{gi}^{(0)}) \\ & + \sum_{i \in \mathcal{G}^-} \left[(1 - \hat{\omega}_{1i}^{(k)})\hat{\lambda}_{2i}^{(k)} - (1 - \hat{\omega}_{2i}^{(k)})\hat{\lambda}_{1i} \right] (P_{gi}^{(0)} - \hat{P}_{gi}^{(0)}) \end{aligned} \tag{33}$$

where $\mathcal{G}^-$ is the set of online generators excluding the reference bus, $\lambda_{1i}^{(k)}$, $\lambda_{2i}^{(k)}$, $\lambda_3^{(k)}$ are the dual variables of constraints (30b), (30c), (30d) respectively. Symbol $\hat{(\cdot)}$ means the correspond parameter is a fixed value.

Master problem In the master problem, we include all variables and constraints for the OPF problem of base case and the Benders' cuts generated by all subproblems.

$$\begin{aligned} \min_{P_{gi}^{(0)}} \quad & C(P_{gi}^{(0)}) && (34) \\ s.t. \quad & P_{gi}^{(0)} - P_{di}^{(0)} = \sum_{(i,j) \in \mathcal{L}} B_{ij}(\theta_i^{(0)} - \theta_j^{(0)}), && i \in \mathcal{N} \\ & |B_{ij}(\theta_i^{(0)} - \theta_j^{(0)})| \leq F_{ij}^{\max} && (i,j) \in \mathcal{L} \\ & P_{gi}^{\min} \leq P_{gi}^{(0)} \leq P_{gi}^{\max} \\ & \theta_{\text{ref}}^{(0)} = 0 \\ & \text{Benders Cuts generated: (33)} \end{aligned}$$

The solution $P_{gi}^{(0)}$ from the master problem is denoted as $\hat{P}_{gi}^{(0)}$ and sent to subproblems. The subproblems further create feasibility cuts for the master problem until the subproblems no longer generate cuts.

IV. Case studies

In this section, we present the case study results. Our numerical experiments are conducted on an Inter(R) Core(TM) i5-8250U CPU @ 1.60 GHZ computer. All presented methods are implemented on Matlab 2019b using CVX and applying Mosek 9.0 as the main solver. To avoid too long time solving for MIP problem, we set the relative optimality tolerance of the Mosek integer optimizer as 1×10^{-3} (default:1×10^{-4}), and the maximum solving time of Mosek as 2000 seconds. All the other configurations are default. The feasibility check tolerance is $\epsilon = 10^{-3}$ for all Benders' methods. For all big-M based methods, M is fixed as 1000.

For convenience, the big-M method based on the formulation (14) is notated as "Method 1" in Tables and Figures; the proposed bilinear formulation and Benders' decomposition Approach 2 is notated as "Method 2".

As the proposed method is based on the parallel computation, its computation time is calculated according to the following equations:

$$T = \sum_{i \in l} \max_{j \in c}(t_i^j)$$

where, T means the total computation time, c is the set of contingency index, l is the set of iteration sequence, t_i^j means the time consumed for the j^{th} contingency at the i^{th} iteration.

For an SCOPF problem, some conflicting contingencies may exist. Those contingencies can not co-exist in the contingencies sets of SCOPF problem [**?**], which means the constraints of these contingencies can not be satisfied simultaneously for the base case. They will cause the SCOPF problem result in infeasible solutions. In this paper, we identified and removed all conflicting contingencies in the test cases. Indeed, research has been conducted to find usable information from these conflicting contingencies, such as the possible system set points to minimize the constraints violations or minimize the load shedding costs. The methodology for this analysis and related works can be found in [**?**].

The identified conflicting contingencies are listed in Table II.

TABLE II
CONFLICT CONTINGENCIES IN ALL CASES.

Cases	**Conflicting contingencies**
Case3	None
Case5	G_3
Case14	None
case39	$G_{31}, G_{32}, G_{33}, G_{34}, G_{35}, G_{36}, L_{1-2}$ $L_{1-39}, L_{2-30}, L_{4-14}, L_{6-11}, L_{6-31}, L_{10-11}$ $L_{10-13}, L_{10-32}, L_{13-14}, L_{16-19}, L_{17-18}, L_{19-20}$ $L_{19-33}, L_{20-34}, L_{21-22}, L_{22-35}, L_{23-36}, L_{25-26}$ $L_{25-37}, L_{26-27}, L_{29-38}$
case118	$L_{85-86}, L_{110-111}, L_{68-116}, L_{12-117}$

A. Three-bus system

In this subsection, we show that the proposed method (Method 2) is capable of correctly reflecting the generator response based on its post-contingency response constraints (13). The testbed system is a three-bus three-machine system. The topology of the system is presented in Fig. 4. The parameters of the branches and generators are listed in Table III.

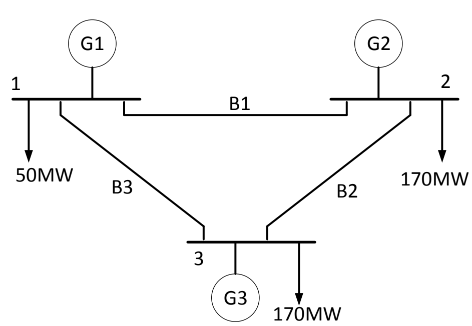

Fig. 4. Topology of the three-bus system.

In the fist experiment, load varying is treated as contingency scenarios. Outage is not considered. Total 7 contingency scenarios are considered in the SCOPF problem. Fig. 5 presents the generator post-contingency responses. The x-axis is the

TABLE III
THREE-BUS SYSTEM PARAMETERS.

	C_2	C_1	C_0	$P_{\max}$	$P_{\min}$	α
G_1	0.11	5	150	3000	0	$1/30$
G_2	0.085	1.2	100	300	0	$1/3$
G_3	0.055	1	50	400	0	$19/30$
B_1, B_2, B_3	$X = 0.0504$ pu			$F_{\max} = 3$ pu		

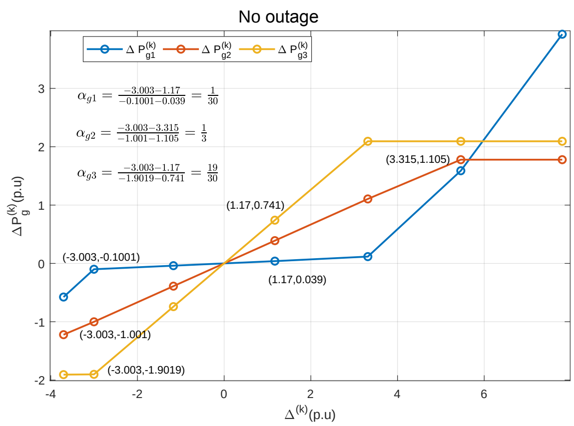

Fig. 5. Generators responses for load variation. G2 and G3 comply with the feasible regions defined by the participation factor, low and upper bounds.

load change against the base case load level. The y-axis notates the variation in generator power against the base case generation. It can be seen that the responses of G2 and G3 comply with the feasible region defined by the participation factor, lower and upper limits. On the other hand, G1 is the reference generator. When either one of the other two generators hit the limit, G1 will no longer assume the designed participation factor of $1/30$.

In the second experiment, $N-1$ contingencies are considered. There are 6 contingencies (3 generator outages, and 3 branch outages). We assume that the reference generator (G1) never fails in any scenario. So only 5 contingencies will be considered in this example.

This SCOPF is solved by the proposed method (Method 2) and the off-shelf solver (Mosek) via big-M formulation (Method 1). Comparison is made on the solution and the computing time. The solution results are listed in Table IV. The results show the objective value for the two methods are the same. The computation time of the big-M method is slightly less than the proposed method. This is due to the small-size of the system. The advantage of the proposed method on computation efficiency will be demonstrated for larger-scale power grids. This point will be validated using an 118-bus system.

TABLE IV
COMPARISON OF OBJECTIVE VALUES FOR THE BIG-M METHOD AND THE PROPOSED METHOD.

	Load Variation	N-1 Contingency
Method 1 obj	4946.17	4946.17
Method 2 obj	4946.17	4946.17

Table V lists the solutions for the second SCOPF problem (the second experiment). In all branch outage scenarios, the generator power outputs in post-contingency are the same as those in the base case. In a contingent scenario with G2 outage, the set of the online generators included G1 and G3. Due to the loss of G2, the change of total is 1.2219 pu. G1 and G3 now share the total power generation change according to their participation factors: $1/30 : 19/30 = 5\% : 95\%$. Hence G1 is expected to share 5% $\left(= \frac{0.8326-0.7715}{1.2219}\right)$ of the total power change, while G3 is expected to share 95% $\left(= \frac{3.0674-0.7715}{1.2219}\right)$. The solution matches the expected results.

For G3 outage, $\Delta^{(k)} = 1.9066$ pu. G1 and G2 share the power change according to their participation factors: $1/30 : 1/3 = 1 : 10$. The solution shows that the power increase of G1 is $0.9448 - 0.7715 = 0.1733$ and the power increase of G2 is $2.9552 - 1.2219 = 1.7333$. Hence, the generators respond as expected for post contingency.

TABLE V
SOLUTION FOR THE N-1 CONTINGENCY SCOPF

	Base case	G2 outage	G3 outage	All branch outage
P_{g1}	0.7715	0.8326	0.9448	0.7715
P_{g2}	1.2219	–	2.9552	1.2219
P_{g3}	1.9066	3.0674	–	1.9066

B. IEEE 118-bus system

Data of the IEEE 118-bus system are from MATPOWER [?]. The line flow limit is set to 500 MVA. In all tests, 100% load means the total load is 42.42 pu. This system consists of 186 branches and 54 generators. Thus, based on "N-1" criterion, there could be 240 contingencies. Part of the contingencies are selected for SCOPF. The information of the selected contingencies is listed in Table VI. Eight critical contingencies, identified by [?], [?], are included in all situations. The rest are randomly selected.

TABLE VI
IEEE 118-BUS SYSTEM CONTINGENCY INFORMATION.

Number of selected contingency	Number of Branch contingency	Number of Generator contingency
8	4	4
20	10	10
30	15	15
40	20	20
50	25	25
Critical contingencies		
$L_{26-30}, L_{34-37}, L_{38-37}, L_{70-71}$ $G_{65}, G_{66}, G_{80}, G_{89}$		

Fig. 6 presents the lower bound computed by the master problem and the maximum of the solutions from subproblems associate with contingency scenarios, along with the iteration. It can be seen that the lower bound converges when all subproblems become feasible. The tested example is the 118 bus system with 190% load.

The computation time of two methods are presented in Figs. 7 and 8. Fig. 7 presents computing time versus loading level for three SCOPF problems which include 8, 30, 50 contingencies respectively. It can be found that for majority of the loading levels, Method 2's computing time is two orders less than Method 1's. Fig. 8 presents computing time versus the number of contingencies. It can be found that while for Method 1, computing time increases linearly as the number of contingency increases, computing time for Method 2 is always less than 10 seconds.

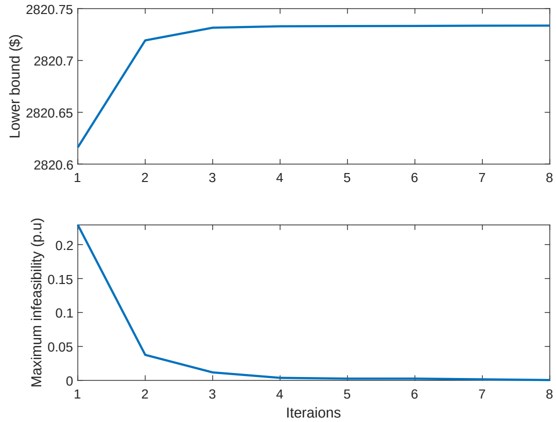

Fig. 6. Lower bound computed from the master problem converges while and the maximum of the subproblem solutions converges to zero. The test case is the IEEE 118-bus system with 190% load.

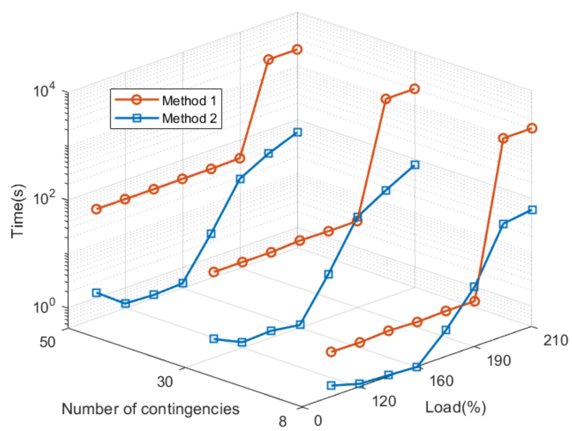

Fig. 7. Computation time against load level.

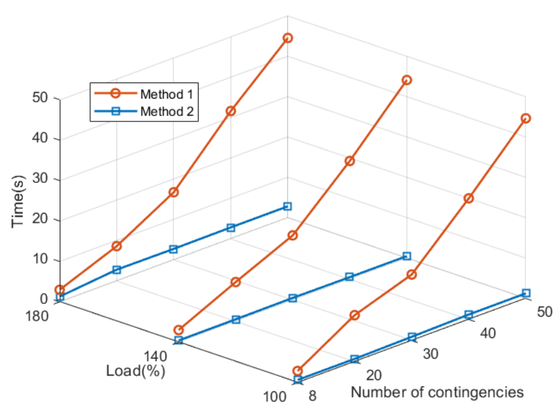

Fig. 8. Computation time against contingency number.

C. Other instances

As a total, five test systems have been examined. Case3 and Case118 have been discussed in the previous subsections. The rest three instances, Case5, Case14, and Case39, are from the MATPOWER case library. The total load of Case3 is set as 3.51

p.u. For Case14, line flow limit 100 MW is imposed. For each instance, the participation factors of generators are defined as a set of fixed positive values with their sum as 1. Table VII presents the information of the three test cases solved by the two methods. In Table VII, the NAN result means that the correspond methods failed to find reasonable solution within a time limit.

For Case3 and Case5, the two methods results the same solution. For Case14, Case39, Case118, as the problem dimension increases, Method 2 becomes more computing efficient compared to Method 1. The solution of Case39 is NAN. This means that the big-M formulation and Mosek solver can not find a reasonable solution within the time limits of 2000 seconds.

TABLE VII
COMPARISON IN DIFFERENT METHODS

Case	# of contingencies	# of binary	Method	Obj	Time	Iteration
Case3	5	16	Method 1	4128.20	0.14	–
			Method 2	4128.20	0.55	1
Case5	9	66	Method 1	22869.60	1.59	–
			Method 2	22869.60	2.56	5
Case14	24	184	Method 1	8459.71	34.36	–
			Method 2	8459.71	1.98	3
Case39	27	480	Method 1	NAN	2000	–
			Method 2	41945.24	5.72	5
Case118	235	24804	Method 1	130508.80	1143.39	–
			Method 2	130508.70	3.89	3

V. CONCLUSION

This paper proposes a bilinear mixed integer programming formulation and an efficient solving approach for security constrained DCOPF to consider generators' post-contingency responses. Through preserving bilinear expressions related to the base case power generation while relaxing the rest bilinear expressions via McCormick envelops, we designed a Benders' decomposition strategy that yields to efficient solving. Case study results demonstrate the efficiency of the proposed formulation compared to the state-of-the-art formulations. In the future work, the proposed method will be implemented based on more general system conditions. Moreover, because the AGC formulation is only related to a generator's real power dispatch, it could be easily adapted to a convex relaxed AC-SCOPF as future work.

REFERENCES

[1] F. Capitanescu, J. M. Ramos, P. Panciatici, D. Kirschen, A. M. Marcolini, L. Platbrood, and L. Wehenkel, "State-of-the-art, challenges, and future trends in security constrained optimal power flow," *Electric Power Systems Research*, vol. 81, no. 8, pp. 1731–1741, 2011.

[2] O. Alsac and B. Stott, "Optimal load flow with steady-state security," *IEEE transactions on power apparatus and systems*, no. 3, pp. 745–751, 1974.

[3] T. Sennewald, F. Sass, and D. Westermann, "A preventive security constrained optimal power flow for mixed ac-hvdc-systems," 2017.

[4] F. Capitanescu, M. Glavic, D. Ernst, and L. Wehenkel, "Applications of security-constrained optimal power flows," in *In Proceedings of Modern Electric Power Systems Symposium, MEPS06*, 2006.

[5] V. Hinojosa and F. Gonzalez-Longatt, "Preventive security-constrained dcopf formulation using power transmission distribution factors and line outage distribution factors," *Energies*, vol. 11, no. 6, p. 1497, 2018.

[6] Y. Yang and Y. Feng, "Large-scale preventive security constrained optimal power flow based on compensation method," in *2015 IEEE Power & Energy Society General Meeting*. IEEE, 2015, pp. 1–5.

[7] Y. Xu, Z. Y. Dong, R. Zhang, K. P. Wong, and M. Lai, "Solving preventive-corrective scopf by a hybrid computational strategy," *IEEE Transactions on Power Systems*, vol. 29, no. 3, pp. 1345–1355, 2013.

[8] Y. Wen and C. Guo, “Discussion on solving preventive-corrective scopf by a hybrid computational strategy,” *IEEE Transactions on Power Systems*, vol. 29, no. 6, pp. 3124–3124, 2014.

[9] L. Roald, F. Oldewurtel, T. Krause, and G. Andersson, “Analytical reformulation of security constrained optimal power flow with probabilistic constraints,” in *2013 IEEE Grenoble Conference*. IEEE, 2013, pp. 1–6.

[10] K. Sundar, H. Nagarajan, L. Roald, S. Misra, R. Bent, and D. Bienstock, “Chance-constrained unit commitment with n-1 security and wind uncertainty,” *IEEE Transactions on Control of Network Systems*, 2019.

[11] M. Velay, M. Vinyals, Y. Besanger, and N. Retiere, “Fully distributed security constrained optimal power flow with primary frequency control,” *International Journal of Electrical Power & Energy Systems*, vol. 110, pp. 536–547, 2019.

[12] R. Madani, M. Ashraphijuo, and J. Lavaei, “Promises of conic relaxation for contingency-constrained optimal power flow problem,” *IEEE Transactions on Power Systems*, vol. 31, no. 2, pp. 1297–1307, 2015.

[13] B. Dandurand and K. Kim, “Scalable decomposition methods for preventive security-constrained optimal power flow,” in *2018 Power Systems Computation Conference (PSCC)*. IEEE, 2018, pp. 1–7.

[14] M. Carrión, Y. Dvorkin, and H. Pandžić, “Primary frequency response in capacity expansion with energy storage,” *IEEE Transactions on Power Systems*, vol. 33, no. 2, pp. 1824–1835, 2017.

[15] Y. Dvorkin, P. Henneaux, D. S. Kirschen, and H. Pandžić, “Optimizing primary response in preventive security-constrained optimal power flow,” *IEEE Systems Journal*, vol. 12, no. 1, pp. 414–423, 2016.

[16] D. Phan and J. Kalagnanam, “Some efficient optimization methods for solving the security-constrained optimal power flow problem,” *IEEE Transactions on Power Systems*, vol. 29, no. 2, pp. 863–872, 2013.

[17] L. Liu, A. Khodaei, W. Yin, and Z. Han, “A distribute parallel approach for big data scale optimal power flow with security constraints,” in *2013 IEEE International Conference on Smart Grid Communications (SmartGridComm)*. IEEE, 2013, pp. 774–778.

[18] S. Chakrabarti, M. Kraning, E. Chu, R. Baldick, and S. Boyd, “Security constrained optimal power flow via proximal message passing,” in *2014 Clemson University Power Systems Conference*. IEEE, 2014, pp. 1–8.

[19] A. Monticelli, M. Pereira, and S. Granville, “Security-constrained optimal power flow with post-contingency corrective rescheduling,” *IEEE Transactions on Power Systems*, vol. 2, no. 1, pp. 175–180, 1987.

[20] Y. Li and J. D. McCalley, “Decomposed scopf for improving efficiency,” *IEEE Transactions on Power Systems*, vol. 24, no. 1, pp. 494–495, 2008.

[21] G. O. Competition. (2018) SCOPF Problem Formulation: Challenge 1. [Online]. Available: https://gocompetition.energy.gov/sites/default/files/SCOPF_Formulation_GO_Comp_20181114.pdf

[22] B. Zeng, Y. An, and L. Kuznia, “Chance constrained mixed integer program: Bilinear and linear formulations, and benders decomposition,” *arXiv preprint arXiv:1403.7875*, 2014.

[23] Y. Zhang, J. Wang, B. Zeng, and Z. Hu, “Chance-constrained two-stage unit commitment under uncertain load and wind power output using bilinear benders decomposition,” *IEEE Transactions on Power Systems*, vol. 32, no. 5, pp. 3637–3647, 2017.

[24] H. Haghighat and B. Zeng, “Stochastic and chance-constrained conic distribution system expansion planning using bilinear benders decomposition,” *IEEE Transactions on Power Systems*, vol. 33, no. 3, pp. 2696–2705, 2017.

[25] Y. Wen, C. Guo, H. Pandžić, and D. S. Kirschen, “Enhanced security-constrained unit commitment with emerging utility-scale energy storage,” *IEEE Transactions on power Systems*, vol. 31, no. 1, pp. 652–662, 2015.

[26] Q. Jiang and K. Xu, “A novel iterative contingency filtering approach to corrective security-constrained optimal power flow,” *IEEE Transactions on Power Systems*, vol. 29, no. 3, pp. 1099–1109, 2013.

[27] F. Capitanescu, “Approaches to obtain usable solutions for infeasible security-constrained optimal power flow problems due to conflicting contingencies,” in *2019 IEEE Milan PowerTech*. IEEE, 2019, pp. 1–6.

[28] R. D. Zimmerman, C. E. Murillo-Sánchez, and R. J. Thomas, “Matpower: Steady-state operations, planning, and analysis tools for power systems research and education,” *IEEE Transactions on power systems*, vol. 26, no. 1, pp. 12–19, 2010.

[29] F. Karbalaei, H. Shahbazi, and M. Mahdavi, “A new method for solving preventive security-constrained optimal power flow based on linear network compression,” *International Journal of Electrical Power & Energy Systems*, vol. 96, pp. 23–29, 2018.

Minyue Ma obtained his B.S. degree from Huazhong University of Science and Technology (Wuhan, China) in 2013. He obtained his M.S. Degree from University of South Florida in 2015. Currently, he is a Ph.D. candidate at University of South Florida, Tampa. His research interests include optimization of power systems.

Lingling Fan is a full professor at University of South Florida, Tampa. Her research interests include control and optimization of power systems and power electronics. Dr. Fan serves as an editor for IEEE Trans. Energy Conversion.